Transcriptomic Analysis of Circular RNA as Potential Biomarkers in Diagnosing Atopic Dermatitis

Xuesong Xiang[1], Chang Liu[1], Huihuang He[1], Wenhong Qiu[1] and Kaiwen Guo[2]

[1]*Department of Immunology, School of Medicine, Jianghan University, Wuhan, China*
[2]*Department of Pathogen Biology, School of Medicine, Wuhan University of Science and Technology, Wuhan, China*

ABSTRACT

Objective: To investigate the functional role of circular RNAs (circRNAs) in atopic dermatitis (AD) and discover potential biomarkers for improved diagnosis and treatment.

Study Design: Descriptive analytical study.

Place and Duration of the Study: Department of Immunology, School of Medicine, Jianghan University, Wuhan, China, from June 2023 to February 2025.

Methodology: Peripheral blood specimens were collected from AD patients and healthy controls; RNA sequencing was performed to assess circRNA expression patterns. Hub genes implicated in AD were identified through gene annotation, protein-protein interaction (PPI) networks, Lasso regression, and random forest algorithms. The expression levels of these hub genes were subsequently confirmed using qRT-PCR.

Results: A total of 151 differentially expressed circRNAs were identified, among which 37 were associated with AD-related genes. Through bioinformatics analysis, six hub genes (*MYD88*, *SIRT1*, *RPS3A*, *DTYMK*, *DDX49*, and *SKP1*) were identified as being closely related to AD.

Conclusion: The findings suggest that *MYD88*, *SIRT1*, *RPS3A*, *DTYMK*, *DDX49*, and *SKP1* can act as promising biomarkers for AD. ROC curve analysis underscored their robust diagnostic capabilities, emphasising their potential utility in early AD detection and treatment evaluation.

Key Words: *Circular RNA, Atopic dermatitis, Lasso regression model, Random forest model.*

How to cite this article: Xiang X, Liu C, He H, Qiu W, Guo K. Transcriptomic Analysis of Circular RNA as Potential Biomarkers in Diagnosing Atopic Dermatitis. *J Coll Physicians Surg Pak* 2025; **35(09)**:1088-1095.

INTRODUCTION

Atopic dermatitis (AD) is a chronic inflammatory skin condition marked by xerosis, severe pruritus, and eczematous lesions.[1] It profoundly affects the quality of life and is frequently linked to sleep disorders, depressive symptoms, and anxiety.[2] The aetiology of AD encompasses IgE-mediated type I hypersensitivity, dominant Th2 immune response (characterised by IL-4/IL-5/IL-13 overproduction), genetic susceptibility (particularly FLG and SPINK5 mutations), environmental triggers, and epidermal barrier dysfunction, with complex interactions between these factors.[3] Nevertheless, the absence of reliable molecular biomarkers poses a challenge to the advancement of precise diagnostic and therapeutic approaches.

Correspondence to: Dr. Wenhong Qiu, Department of Immunology, School of Medicine, Jianghan University, Wuhan, Hubei, China
E-mail: qiuwenhong@jhun.edu.cn

Received: February 21, 2025; Revised: July 22, 2025; Accepted: August 05, 2025
DOI: https://doi.org/10.29271/jcpsp.2025.09.1088

Circular RNAs (circRNAs), a category of non-coding RNAs comprising covalently closed-loop structures, have gained recognition as pivotal modulators of gene expression owing to their high stability, evolutionary conservation, and tissue-specific expression patterns.[4] Although circRNAs participate in immune modulation and inflammatory processes across various diseases, their involvement in AD remains largely unexplored.

This study aimed to elucidate the functional significance of circRNAs in AD pathogenesis and to establish novel molecular biomarkers for clinical application. The investigation was particularly intended to focus on characterising the diagnostic potential of circRNA signatures and their therapeutic implications for precision medicine in AD management.

METHODOLOGY

This analytical study was conducted at the Department of Immunology, School of Medicine, Jianghan University, Wuhan, China, from June 2023 to February 2025. Peripheral blood samples were collected from three AD patients and three healthy controls for circRNA expression profiling. AD patients were recruited based on established diagnostic criteria,[5-7] with inclusion criteria as follows: compliance with Williams' diagnostic criteria,[7] no topical medication use within one week

before blood collection, and no AD-related systemic treatment within two weeks prior to blood sampling. Exclusion criteria included conditions such as drug-induced eruption, hyper-IgE syndrome, malignant eosinophilia, skin infections, connective tissue diseases, and malignancies, which could confound the results. Healthy controls were defined as individuals without AD or other chronic skin diseases. All participants were of Han Chinese ethnicity, and the research adhered rigorously to ethical standards, with approval granted by the Medical Ethics Committee of Sixth Hospital, Wuhan, China (Approval No. WHSHIRB-K-2023009). Informed consent was obtained from all participants included in the study. Demographic information, SCORAD scores, and EASI scores for both patients and healthy individuals were summarised in Table I. The sample size for the initial exploratory phase was determined based on practical considerations, including resource availability and the feasibility of recruiting well-characterised AD patients. This pilot study aimed to optimise experimental protocols and identify potential circRNA candidates for further investigation. The findings from this phase were subsequently validated using a larger independent cohort from a public database to ensure the robustness of the results.

Table I: Clinical characteristics of AD patients and health controls.

Characteristics	Patients (n = 3)	Controls (n = 3)
Gender: male	3 (100)	3 (100)
Age (years), mean ± SD	30.3 ± 22.1	38.3 ± 14.0
Body mass index (kg/m2), mean ± SD	22.1 ± 1.67	22.0 ± 0.87
SCORAD	30.2 ± 9.8	-
EASI, mean ± SD	20.7 ± 10.2	-
An itchy skin condition (major criterion)	3 (100)	-
History of skin creases involvement*	3 (100)	-
A personal history of asthma or hay fever*	1 (33.3)	-
A history of general dry skin in the last year*	3 (100)	-
Visible flexural eczema*	3 (100)	-
Onset under the age of 2 years (not used if child aged under 4 years)*	1 (33.3)	-
Topical corticosteroid therapy at baseline	0	-

*Fulfilment of the major criterion with three or more minor criteria was required for the diagnosis of AD. *Minor criteria. Data are presented as nos. (%) unless otherwise indicated; — Not applicable (healthy controls did not undergo disease-specific assessments).*

Peripheral blood specimens were selected for circRNA profiling due to their ease of collection, non-invasive nature, and suitability for large-scale screening and clinical applications. As a critical component of liquid biopsy, peripheral blood reflects systemic inflammation and immune responses, making it highly valuable for clinical translation. High-throughput sequencing was utilised to examine circRNA expression in peripheral blood, providing insights into the pathological mechanisms underlying AD and the potential utility of circRNAs as diagnostic and therapeutic biomarkers.

Total RNA was isolated from peripheral blood samples using TRIzol reagent (15596018CN), and its concentration and purity were assessed to ensure sample integrity. RNA samples underwent high-throughput sequencing on the Illumina HiSeq platform, generating transcriptomic data for both AD patients and healthy controls. Raw data were stored in FASTQ format, containing sequencing reads and corresponding quality metrics.

To ensure data quality for downstream analysis, FastQC (version 0.11.2; https://www.bioinformatics.babraham.ac.uk/projects/fastqc/) was employed to evaluate raw sequencing data and to assess parameters such as read length, base distribution, and error rates. Low-quality reads were filtered using the Trimmomatic (version 0.39; https://www.usadellab.org/cms/index.php?page=trimmomatic), which removed adapter sequences and low-quality bases to yield high-quality clean data.[8]

For alignment, BWA-MEM (version 1.5; https://github.com/lh3/bwa) was utilised to map high-quality sequencing reads to the reference genome, determining the positional information of each sequence.[9] CIRI2 (version 2.06) was employed to identify circRNAs and quantify their expression levels. BED tools (version 2.26.0; https://github.com/arq5x/bedtools2) was used to annotate the functional characteristics of circRNAs based on their genomic locations and gene annotations.

By comparing transcriptome data between AD patients and healthy controls, significantly differentially expressed circRNAs, miRNAs, and mRNAs were identified. CIRI2 (version 2.06; https://sourceforge.net/projects/ciri/) was applied to detect circRNAs in peripheral blood, and their expression levels were analysed to determine differential expression.[10] DESeq2 (version 1.46.0) in R was employed for data normalisation and statistical significance testing, controlling for technical and experimental biases.

Differentially expressed genes corresponding to mRNAs were imported into the STRING database (https://cn.string-db.org/) to construct a protein-protein interaction (PPI) network. The network was visualised using Cytoscape (https://cytoscape.org/), and topological properties such as degree, centrality, and eigenvector centrality were calculated using the Cytoscape plugin CentiScaPe (version 2.2; https://chianti.ucsd.edu/cyto_web/plugins/index.php) to identify hub genes. These hub genes, central to the PPI network, are likely to play pivotal regulatory roles in AD pathogenesis. To identify potential biomarkers for AD, the GSE32924 dataset (https://www.ncbi.nlm.nih.gov/geo/query/acc.cgi?acc=*GSE32924*) from the Gene Expression Omnibus (GEO) was retrieved. This dataset comprises gene expression profiles from skin tissues of 13 AD patients and 8 healthy controls of East Asian descent. The sample size was determined based on data availability in the public database and is consistent with sample sizes used in similar studies investigating AD biomarkers.[11,12] Differential gene expression analysis was performed using the limma package (version 3.56.2) in R to identify genes significantly associated with AD.[13] The robustness of the findings was further supported by the use of an independent validation cohort and the consistency of results with previous studies.

To validate the consistency and potential roles of these genes across different tissues, the expression patterns of hub genes, previously identified in the PPI network, were further analysed in the GSE32924 dataset. This analysis revealed differential expression of hub genes between peripheral blood and skin samples from AD patients, providing robust evidence for their tissue-specific roles in AD pathogenesis.

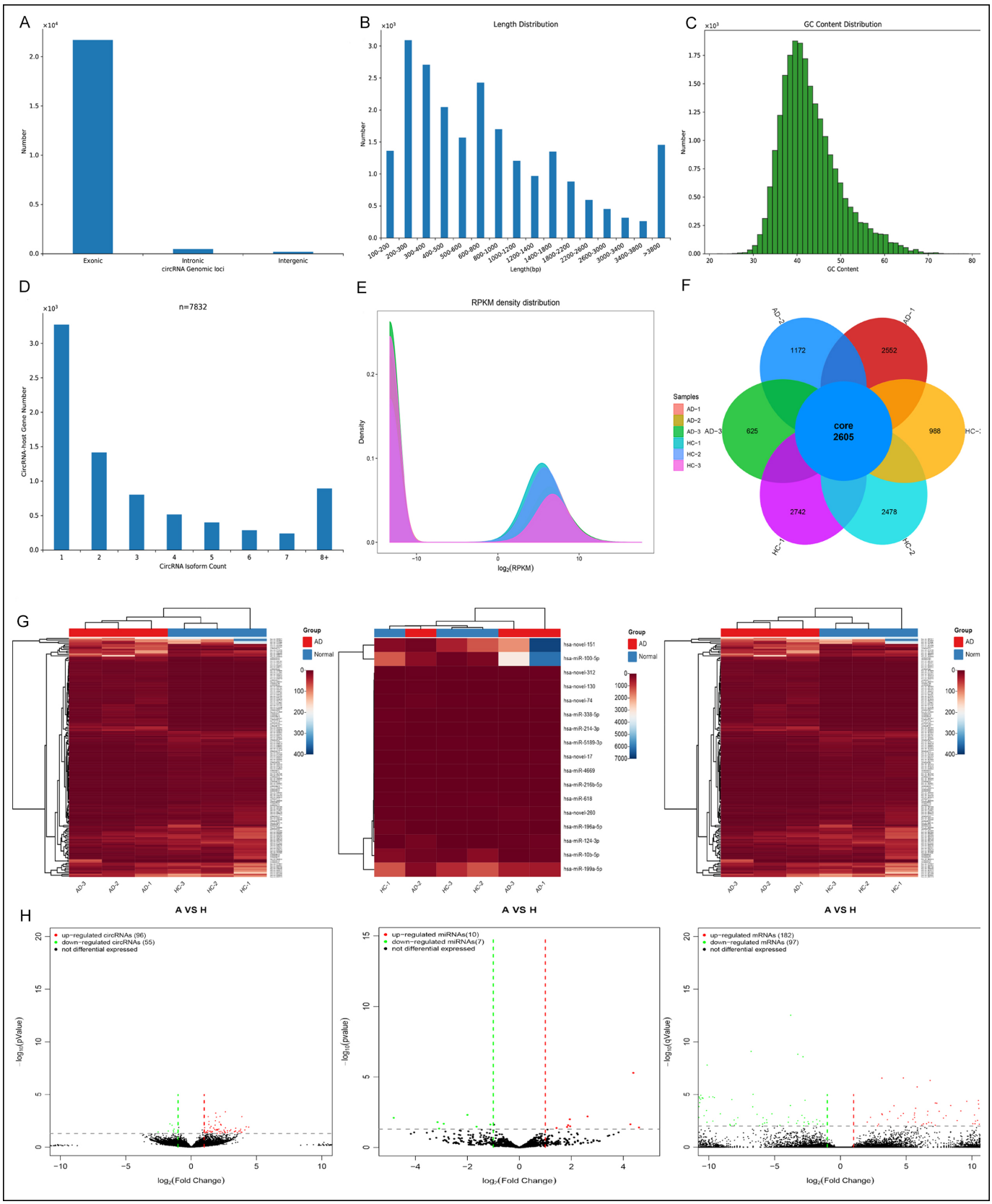

Figure 1: Characteristics of circRNA sequencing in peripheral blood of AD patients and healthy controls. (A) Bar plot of circRNA sources. (B) Length distribution of the circRNAs. (C) GC content distribution of circRNAs. (D) Distribution of the circRNA counts. (E) Density distribution of the circRNA expression. (F) Co-expressed circRNAs. (G) Heatmap of RNA expression differences between AD patients and healthy controls. (H) Volcano plot of the differentially expressed genes.

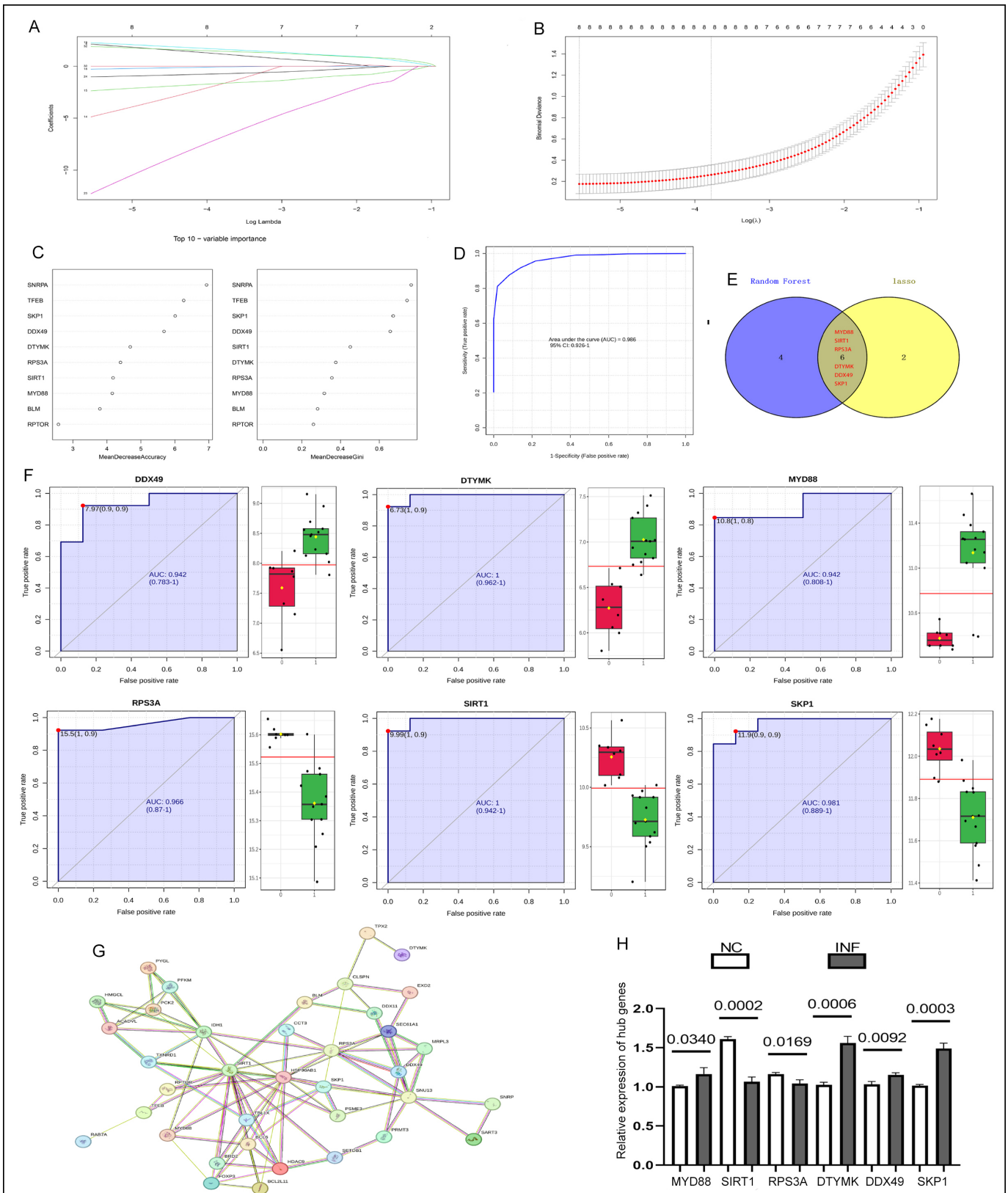

Figure 2: Lasso regression and random forest modelling for AD biomarkers identification and immune infiltration correlation analysis. (A) Lasso regression coefficient path plot. (B) Cross-validation curve for Lasso regression. (C) Top 10 important genes in the random forest model. (D) ROC curve for the random forest model. (E) Intersection of genes selected by Lasso and random forest models. (F) ROC curves and expression levels of the six potential biomarkers in AD patients and healthy controls. (G) Thirty-seven hub genes identified in AD patients. (H) Relative expression of six hub genes in control and inflammatory HaCaT cell models. The data shown in the figure represent p-values determined by t-tests for intergroup comparisons.

To refine the identification of key genes closely linked to AD pathology, Lasso Cox regression analysis was conducted using the glmnet package (version 4.1-8). This penalised regression approach reduced model complexity and highlighted genes with significant impact on AD. Additionally, random forest analysis was performed using the Random Forest package (version 4.7-1.1) to prioritise hub genes most relevant to AD, uncovering potential biomarkers with high diagnostic value.[14]

Finally, the predictive performance of the identified gene models was evaluated by constructing receiver operating characteristic (ROC) curves. These curves assessed the sensitivity and specificity of the models in diagnosing AD, providing a quantitative measure of their clinical utility. HaCaT cells were obtained from ProCell (Cat# CL-0090, Wuhan, China) and cultured in MEM with 10% FBS under standard conditions. To simulate the inflammatory environment associated with AD, a cell-based inflammation model was established by stimulating HaCaT cells with 20 ng/mL TNF-α and 100 μg/mL poly(I:C) for 24 hours.[15] Total RNA was extracted from HaCaT cells using TRIzol reagent (15596018CN), ensuring RNA integrity and purity. Subsequently, cDNA was synthesised using the ReverTra Ace® qRT-PCR RT Kit (FSQ-101) to serve as a template for gene expression analysis.

Quantitative real-time PCR (qRT-PCR) was performed using the MonAmp™ SYBR® Green qRT-PCR Mix (MQ10301S). Fluorescence signals during the PCR process were detected using the CFX96 Real-Time System (Bio-Rad, Shanghai, China), with *GAPDH* as the internal reference gene for normalisation. The relative gene expression levels were calculated using the 2^-ΔΔCt method to ensure accuracy and reliability.[16] Primer sequences were designed with Primer-BLAST (https://www.ncbi.nlm.nih.gov/tools/primer-blast/) to ensure strict specificity to the target gene sequences. The primer sequences were as follows:

MYD88 forward: CTATTGCCCCAGCGACATCC
MYD88 reverse: CGTGGCCTTCTAGCCAACC
SIRT1 forward: TGGGTACCGAGATAACCTTCTG
SIRT1 reverse: TTGTTCGAGGATCTGTGCC
RPS3A forward: AACAGGTCCGCCAAATCCG
RPS3A reverse: AACTTGGGCTTCTTCAGCATT
DTYMK forward: CCGGTGCCAAGGAGTTACAG
DTYMK reverse: ATGAGCTGGTGGAAACACCG
DDX49 forward: TCGTGGCTCGTGGAACAAT
DDX49 reverse: GTCTTAGCACAGCCCAAGCA
SKP1 forward: CCTGAAAGTTGACCAAGGAACAC
SKP1 reverse: TGGGCTTCCTCCTCTTCAGTA
GAPDH forward: AATTCCATGGCACCGTCAAG
GAPDH reverse: AGCATCGCCCCACTTGATTT

Differential expression analysis between healthy controls and AD patients was performed using the limma package (version 3.56.2), with |logFC| ≥1 and p <0.05 as the criteria for identifying significant differentially expressed genes. Prior to analysis, the assumption of normality was checked using the Shapiro-Wilk test. The results indicated that most of the data for both groups satisfied the normality assumption (p >0.05); however, a small proportion of genes exhibited non-normal distributions (p ≤0.05). In cases where the normality assumption was violated, data were log-transformed to meet the assumption. For differential expression analysis of circRNAs and miRNAs, the DEGseq2 package (version 1.46.0) was used, with a significance threshold set at p <0.05 and |log2FC| >1. For mRNA differential expression analysis, a more stringent criterion was applied, with q <0.01 and |log2FC| >1 considered significant.

To evaluate the predictive performance of potential biomarkers, ROC curves were plotted using MetaboAnalyst 5.0 (https://www.metaboanalyst.ca/), and the area under the curve (AUC) was calculated. Additionally, intergroup differences in qRT-PCR experiments were analysed using t-tests in GraphPad Prism 8, with p <0.05 considered statistically significant.

RESULTS

The sequencing results are presented in Figure 1A-H. The majority of circRNAs were derived from exon regions, indicating that exons are the primary source of circRNA formation. The length distribution of circRNAs was predominantly between 200 and 800 nucleotides, demonstrating a stable length characteristic. The GC content of circRNAs was concentrated around 40%, reflecting a relatively uniform sequence feature. Co-expression analysis identified 2,605 circRNAs shared across different samples, suggesting their stability and conservation.

In terms of expression levels and density, circRNAs in healthy controls exhibited relatively low expression levels and high-density distribution, whereas circRNAs in AD patients showed significantly elevated expression levels but lower density distribution.

Differential expression analysis identified 151 circRNAs (96 upregulated and 55 downregulated), 17 miRNAs (10 upregulated and 7 downregulated), and 279 mRNAs (182 upregulated and 97 downregulated) that exhibited significant differential expression between AD patients and healthy controls. These differentially expressed molecules were visualised using a heatmap and volcano plot (Figure 1G, H).

Based on differentially expressed mRNAs from RNA sequencing, a PPI network for AD was constructed using the STRING database (https://string-db.org/). Visualisation with Cytoscape revealed a network comprising 246 differentially expressed genes (236 nodes and 261 edges), with a PPI enrichment p <0.05, indicating significant biological relevance. Topological analysis using the CentiScaPe plugin identified 37 hub genes with high connectivity and centrality (Figure 2G), suggesting their potential core regulatory roles in AD pathogenesis.

To further investigate the roles of hub genes in AD, differential gene expression analysis was conducted on the GSE32924 dataset using the limma package, which confirmed significant differential expression of the 37 hub genes. Lasso regression and random forest models were employed for feature selection and importance ranking (Figure 2A-D). Cross-validation (Figure 2E) and ROC curve analysis identified six hub genes (*MYD88*, *SIRT1*, *RPS3A*, *DTYMK*, *DDX49*, and *SKP1*) with high diagnostic performance (AUC values close to 1, Figure 2F), suggesting their potential as diagnostic biomarkers for AD.

qRT-PCR results demonstrated significant changes in the expression of the six hub genes in HaCaT cells stimulated with 20 ng/mL TNF-α and 100 μg/mL poly(I:C) for 24 hours (Figure 2H). *MYD88* ($p = 0.0340$), *DTYMK* ($p = 0.0006$), *DDX49* ($p = 0.0092$), and *SKP1* ($p = 0.0003$) were significantly upregulated, while *SIRT1* ($p = 0.0002$) and *RPS3A* ($p = 0.0169$) were significantly downregulated. The findings were consistent with prior predictions and supported their roles in the inflammatory responses and AD. These results validate the abnormal expression of the six hub genes in inflammatory responses, highlighting their potential roles in AD and other inflammation-related diseases.

DISCUSSION

AD is a prevalent chronic inflammatory skin disorder characterised by persistent pruritus and recurrent eczematous lesions. Its global prevalence is increasing, particularly among paediatric populations. AD not only impacts physical health but is also linked to psychological comorbidities, including sleep disturbances, depressive symptoms, and anxiety, significantly diminishing the quality of life.[17,18] Although genetic predisposition and environmental triggers have been implicated in the pathogenesis of AD, its precise aetiology and pathological mechanisms remain incompletely elucidated. Current research highlights the critical roles of immune dysregulation, IgE-mediated immune responses, and epidermal barrier dysfunction in the development and progression of AD.[19]

This study represents the first systematic analysis of circRNA expression profiles in the peripheral blood of AD patients using RNA sequencing. The study successfully identified differentially expressed circRNAs, miRNAs, and mRNAs closely associated with AD. Specifically, 151 circRNAs (96 upregulated and 55 downregulated), 17 miRNAs (10 upregulated and 7 downregulated), and 279 mRNAs (182 upregulated and 97 downregulated) were identified, which may play pivotal roles in the pathogenesis of AD. Through integrated analysis, these findings provide novel molecular insights into the pathophysiological processes of AD and offer potential biomarkers and therapeutic strategies for its diagnosis and management.

Through constructing a PPI network and performing model analysis, six hub genes with high diagnostic potential were identified: *MYD88*, *SIRT1*, *RPS3A*, *DTYMK*, *DDX49*, and *SKP1*. These genes were further validated using qRT-PCR in a HaCaT cell model. The six hub genes exhibited significant differential expression in both the peripheral blood of AD patients and skin samples from the GEO dataset, underscoring their stability and reliability as potential biomarkers. *MYD88*, a core component of the Toll-like receptor signalling pathway, regulates inflammatory responses, and its aberrant expression may lead to T-cell and mast cell activation.[20] *SIRT1* modulates the expression of inflammatory factors through deacetylation, and its dysregulation may contribute to immune cell dysfunction.[21] *RPS3A*, a ribosomal protein involved in protein synthesis, influences immune cell function.[22] *DTYMK* and *DDX49* are implicated in DNA damage repair and RNA metabolism, respectively, potentially affecting immune cell function and signal transduction.[23,24] *SKP1*, a component of the ubiquitin ligase complex, regulates protein degradation and participates in maintaining protein homeostasis in immune cells.[25]

The diagnostic performance of these biomarkers showed exceptional accuracy in ROC analysis: *DTYMK* (AUC = 1.0, 95% CI: 0.962-1), and *SIRT1* (AUC = 1.0, CI: 0.942-1) achieved perfect discrimination, while *SKP1* (AUC = 0.981, CI: 0.889-1), *RPS3A* (AUC = 0.966, CI: 0.87-1), *MYD88* (AUC = 0.942, CI: 0.808-1), and *DDX49* (AUC = 0.942, CI: 0.783-1) demonstrated near-perfect classification. Notably, *DTYMK*, *RPS3A*, and *DDX49* have not been previously associated with other inflammatory dermatoses such as psoriasis, suggesting potential AD-specific roles. For *MYD88*, *SIRT1*, and *SKP1* (which are known to participate in multiple inflammatory pathways) the observed co-expression patterns may generate AD-distinctive signatures.

Furthermore, ROC curve analysis demonstrated that these six genes exhibit high diagnostic performance, highlighting their potential clinical utility as biomarkers for AD.

This study is the first to reveal the potential roles and clinical significance of circRNAs and six hub genes in AD. However, there are certain limitations: the sample size was relatively small (3 AD patients and 3 healthy controls), and the generalisability and statistical power of the results require further validation. Future studies should expand the sample size to include AD patients with varying disease severities and genetic backgrounds. Additionally, while qRT-PCR was employed to validate the expression of hub genes, further cell-based and animal model experiments are needed to elucidate their specific functions and regulatory mechanisms.

CONCLUSION

This study analysed circRNA expression profiles in the peripheral blood of AD patients using RNA sequencing and identified six hub genes (*MYD88*, *SIRT1*, *RPS3A*, *DTYMK*, *DDX49*, and *SKP1*) closely associated with AD.

FUNDING:
The study was funded by the National Natural Science Foundation of China (Grant No. 31671092) and the Research Fund of Jianghan University (Grant No. 2023KJZX29). The research performed in this study followed the laws of China and the authors' respective institutions.

ETHICAL APPROVAL:
Ethical approval was obtained from the Medical Ethics Committee of Sixth Hospital, Wuhan, China (Approval No: WHSHIRB-K-2023009).

PATIENTS' CONSENT:
The patients provided their written informed consent form to participate in this study.

COMPETING INTEREST:
The authors declared no conflict of interest.

AUTHORS' CONTRIBUTION:
XX: Conception, data curation, formal analysis, methodology, software, validation, visualisation, and writing of the original draft.
CL, HH: Methodology, writing, review, and editing.
WQ: Supervision, funding acquisition, resources, methodology, review, and editing.
KG: Supervision, resources, methodology, writing, review, and editing.
All authors approved the final version of the manuscript to be published.

REFERENCES

1. Sroka-Tomaszewska J, Trzeciak M. Molecular mechanisms of atopic dermatitis pathogenesis. *Int J Mol Sci* 2021; **22(8)**: 4130. doi: 10.3390/ijms22084130.
2. Bawany F, Northcott CA, Beck LA, Pigeon WR. Sleep disturbances and atopic dermatitis: Relationships, methods for assessment, and therapies. *J Allergy Clin Immunol Pract* 2021; **9(4)**:1488-500. doi: 10.1016/j.jaip.2020.12.007.
3. Tokura Y, Hayano S. Subtypes of atopic dermatitis: From phenotype to endotype. *Allergol Int* 2022; **71(1)**:14-24. doi: 10.1016/j.alit.2021.07.003.
4. Liu R, Zhang L, Zhao X, Liu J, Chang W, Zhou L, *et al*. circRNA: Regulatory factors and potential therapeutic targets in inflammatory dermatoses. *J Cell Mol Med* 2022; **26(16)**:4389-400. doi: 10.1111/jcmm.17473.
5. Jemec GB, Wulf HC. The applicability of clinical scoring systems: SCORAD and PASI in psoriasis and atopic dermatitis. *Acta Derm Venereol* 1997; **77(5)**:392-3. doi: 10.2340/0001555577392393.
6. Chopra R, Vakharia PP, Sacotte R, Patel N, Immaneni S, White T, *et al*. Severity strata for eczema area and severity index (EASI), modified EASI, scoring atopic dermatitis (SCORAD), objective SCORAD, atopic dermatitis severity index and body surface area in adolescents and adults with atopic dermatitis. *Br J Dermatol* 2017; **177(5)**:1316-21. doi: 10.1111/bjd.15641.
7. Gu H, Chen XS, Chen K, Yan Y, Jing H, Chen XQ, *et al*. Evaluation of diagnostic criteria for atopic dermatitis: Validity of the criteria of Williams *et al*. In a hospital-based setting. *Br J Dermatol* 2001; **145(3)**:428-33. doi: 10.1046/j.1365-2133.2001.04379.x.
8. Bolger AM, Lohse M, Usadel B. Trimmomatic: A flexible trimmer for illumina sequence data. *Bioinformatics* 2014; **30(15)**:2114-20. doi: 10.1093/bioinformatics/btu170.
9. Li H. Aligning sequence reads, clone sequences and assembly contigs with BWA-MEM. *Genomics 1303* 2013. doi: 10.48550/arXiv.1303.3997.
10. Gao Y, Zhang J, Zhao F. Circular RNA identification based on multiple seed matching. *Brief Bioinform* 2018; **19(5)**: 803-10. doi: 10.1093/bib/bbx014.
11. Suarez-Farinas M, Tintle SJ, Shemer A, Chiricozzi A, Nograles K, Cardinale I, *et al*. Nonlesional atopic dermatitis skin is characterized by broad terminal differentiation defects and variable immune abnormalities. *J Allergy Clin Immunol* 2011; **127(4)**:954-64.e1-4. doi: 10.1016/j.jaci.2010.12.1124.
12. Zhao W, Jiang H, Gu Y, Zhang W, Bao S, Dai M, *et al*. Fangji Dihuang formulation ameliorated DNCB-induced atopic dermatitis-like skin lesions by IL-17 signaling pathway: Integrating network analysis and experimental validation. *Front Pharmacol* 2023; **14**:1220945. doi: 10.3389/fphar.2023.1220945.
13. Ritchie ME, Phipson B, Wu D, Hu Y, Law CW, Shi W, *et al*. limma powers differential expression analyses for RNA-sequencing and microarray studies. *Nucleic Acids Res* 2015; **43(7)**:e47. doi: 10.1093/nar/gkv007.
14. Breiman L. Random forests. *Machine Learning* 2001; **45**:5-32. doi: 10.1023/A:1010933404324.
15. Yuan W, Chen Y, Zhou Y, Bao K, Yu X, Xu Y, *et al*. Formononetin attenuates atopic dermatitis by upregulating A20 expression *via* activation of G protein-coupled estrogen receptor. *J Ethnopharmacol* 2021; **266**:113397. doi: 10.1016/j.jep.2020.113397.
16. Livak KJ, Schmittgen TD. Analysis of relative gene expression data using real-time quantitative PCR and the $2^{-\Delta\Delta CT}$ method. *Methods* 2001; **25(4)**:402-8. doi: 10.1006/meth.2001.1262.
17. Cheng BT, Silverberg JI. Depression and psychological distress in US adults with atopic dermatitis. *Ann Allergy Asthma Immunol* 2019; **123(2)**:179-85. doi: 10.1016/j.anai.2019.06.002.
18. Yu SH, Attarian H, Zee P, Silverberg JI. Burden of sleep and fatigue in US adults with atopic dermatitis. *Dermatitis* 2016; **27(2)**:50-8. doi: 10.1097/DER.0000000000000161.
19. Laske N, Bunikowski R, Niggemann B. Extraordinarily high serum IgE levels and consequences for atopic phenotypes. *Ann Allergy Asthma Immunol* 2003; **91(2)**:202-4. doi: 10.1016/S1081-1206(10)62178-3.
20. Kim YC, Lee SE, Kim SK, Jang HD, Hwang I, Jin S, *et al*. Toll-like receptor mediated inflammation requires FASN-dependent MYD88 palmitoylation. *Nat Chem Biol* 2019; **15(9)**: 907-16. doi: 10.1038/s41589-019-0344-0.
21. Yang Y, Liu Y, Wang Y, Chao Y, Zhang J, Jia Y, *et al*. Regulation of SIRT1 and its roles in inflammation. *Front Immunol* 2022; **13**:831168. doi: 10.3389/fimmu.2022.831168.

22. Zhou C, Weng J, Liu C, Zhou Q, Chen W, Hsu JL, *et al*. High RPS3A expression correlates with low tumor immune cell infiltration and unfavorable prognosis in hepatocellular carcinoma patients. *Am J Cancer Res* 2020; **10(9)**:2768-84.
23. Zhao H, Xie R, Zhang C, Lu G, Kong H. Pan-cancer analysis of prognostic and immunological role of DTYMK in human tumors. *Front Genet* 2022; **13**:989460. doi: 10.3389/fgene.2022.989460.
24. Awasthi S, Verma M, Mahesh A, K Khan MI, Govindaraju G, Rajavelu A, *et al*. DDX49 is an RNA helicase that affects translation by regulating mRNA export and the levels of preribosomal RNA. *Nucleic Acids Res* 2018; **46(12)**:6304-17. doi: 10.1093/nar/gky231.
25. Xie CM, Wei W, Sun Y. Role of SKP1-CUL1-F-box-protein (SCF) E3 ubiquitin ligases in skin cancer. *J Genet Genomics* 2013; **40(3)**:97-106. doi: 10.1016/j.jgg.2013.02.001.